Molecular Biology of the Cell
Vol. 18, 166–175, January 2007

The Vacuolar Transporter Chaperone (VTC) Complex Is Required for Microautophagy

Andreas Uttenweiler,* Heinz Schwarz,† Heinz Neumann,* and Andreas Mayer*

*Département de Biochimie, Université de Lausanne, 1066 Epalinges, Switzerland; and †Max-Planck-Institut für Entwicklungsbiologie, 72076 Tübingen, Germany

Submitted August 2, 2006; Revised October 10, 2006; Accepted October 20, 2006
Monitoring Editor: Howard Riezman

Microautophagy involves direct invagination and fission of the vacuolar/lysosomal membrane under nutrient limitation. This occurs by an autophagic tube, a specialized vacuolar membrane invagination that pinches off vesicles into the vacuolar lumen. In this study we have identified the VTC (vacuolar transporter chaperone) complex as required for microautophagy. The VTC complex is present on the ER and vacuoles and at the cell periphery. On induction of autophagy by nutrient limitation the VTC complex is recruited to and concentrated on vacuoles. The VTC complex is inhomogeneously distributed within the vacuolar membranes, showing an enrichment on autophagic tubes. Deletion of the VTC complex blocks microautophagic uptake into vacuoles. The mutants still form autophagic tubes but the production of microautophagic vesicles from their tips is impaired. In line with this, affinity-purified antibodies to the Vtc proteins inhibit microautophagic uptake in a reconstituted system in vitro. Our data suggest that the VTC complex is an important constituent of autophagic tubes and that it is required for scission of microautophagic vesicles from these tubes.

INTRODUCTION

Autophagy occurs in all eukaryotic cells (Reggiori and Klionsky, 2002). In yeast it has mainly been characterized as an adaptation to nutrient stress such as nitrogen limitation: during autophagy large portions of cytosolic and membraneous material are delivered to the lysosome (in yeast called vacuole) for degradation and recycling (Takeshige *et al.*, 1992). This phenomenon enables cells to survive long periods of starvation. However, in higher eukaryotes autophagy also plays an important role in developmental changes (Levine and Klionsky, 2004), regulation of lifespan (Bergamini *et al.*, 2003; Longo and Finch, 2003; Melendez *et al.*, 2003; Vellai *et al.*, 2003), cancer (Qu *et al.*, 2003; Yue *et al.*, 2003; Gozuacik and Kimchi, 2004), and in neurodegenerative disorders like Huntington's, Parkinson's, or Alzheimer's disease (Yuan *et al.*, 2003). It is also part of the innate immune system assisting in eliminating intracellular pathogens after infection (Gutierrez *et al.*, 2004; Nakagawa *et al.*, 2004; Ogawa *et al.*, 2005).

Macroautophagy in yeast is defined as the uptake of cytosolic contents by fusion of double-layered vesicles (autophagosomes) with vacuoles (Baba *et al.*, 1994). Autophagosomes originate from a preautophagosomal structure (PAS) in the vicinity of the vacuole and, during their formation, enwrap portions of cytosol. Fusion of the outer autophagosomal layer with the vacuolar membrane liberates autophagic bodies (single-layered intravacuolar vesicles) into the vacuolar lumen for degradation (Takeshige *et al.*, 1992). Relevant actors of macroautophagy (Atg proteins; Klionsky *et al.*, 2003) have been identified, mainly by genetic screens (Tsukada and Ohsumi, 1993; Thumm *et al.*, 1994; Harding *et al.*, 1995, 1996; Titorenko *et al.*, 1995) and have been studied intensively over the last decade.

Little is known about microautophagy, a process consisting of a direct invagination of the vacuolar boundary membrane and budding of autophagic bodies into the vacuolar lumen (Muller *et al.*, 2000; Sattler and Mayer, 2000; Kunz *et al.*, 2004). Microautophagy of soluble cytosolic components is topologically equivalent to invaginations occurring during multivesicular body (MVB) formation at the endosome, piecemeal microautophagy of the nucleus (PMN) (Roberts *et al.*, 2003) into the yeast vacuole and micropexophagy in methylotrophic yeasts (Veenhuis *et al.*, 1983; Tuttle *et al.*, 1993; Tuttle and Dunn, 1995; Sakai *et al.*, 1998; Mukaiyama *et al.*, 2002, 2004). Although microautophagy of soluble components, like macroautophagy, is induced by nitrogen starvation and rapamycin (a pharmacological agent inhibiting Tor kinase signaling) and although pexophagic vacuole invagination depends on Atg proteins (Hutchins *et al.*, 1999; Kim *et al.*, 1999; Yuan *et al.*, 1999; Stromhaug *et al.*, 2001), there is no evidence that Atg proteins are directly involved in either PMN (Roberts *et al.*, 2003) or microautophagic uptake. Macroautophagy seems to be a prerequisite for microautophagy to occur, however (Sattler and Mayer, 2000). Microautophagy is controlled by the TOR and EGO (composed of proteins Ego1p, Gtr2p, and Ego3p) signaling complexes (Dubouloz *et al.*, 2005). It leads to direct uptake and degradation of the vacuolar boundary membrane. Hence the process could compensate the enormous influx of membrane caused by macroautophagy. Based on this evidence, microautophagy appears to be required for the transition from the rapamycin-induced growth arrest to logarithmic growth (Dubouloz *et al.*, 2005) and for maintenance of organellar size and membrane composition rather than for cell survival under nutrient restriction.

Autophagic tubes (microautophagic vacuole invaginations) show dramatically reduced density of transmembrane

This article was published online ahead of print in *MBC in Press* (http://www.molbiolcell.org/cgi/doi/10.1091/mbc.E06–08–0664) on November 1, 2006.

Address correspondence to: Andreas Mayer (andreas.mayer@unil.ch).

Abbreviations used: Cmd1, calmodulin; VTC, vacuolar transporter chaperone.

particles toward their tips, i.e., toward the site where autophagic bodies pinch off into the vacuolar lumen. Microautophagic vesicles share this exceptional ultrastructural feature with nascent autophagosomes (Muller *et al.*, 2000). Also nascent autophagosomes are virtually free of intramembraneous particles, suggesting that membrane removal by microautophagy might compensate macroautophagic membrane influx both in terms of quantity and quality. Microautophagic vacuole invagination could be reconstituted in a cell-free system composed of purified vacuoles and cytosolic extracts (Muller *et al.*, 2000; Sattler and Mayer, 2000). Using a pharmacological approach, the in vitro uptake reaction could be dissected into different kinetic stages (Kunz *et al.*, 2004). According to their ability to block the reaction at different kinetic stages, these inhibitors have been defined as early acting class A inhibitors (nystatin, GTPγS, aristolochic acid) and late acting class B inhibitors (W-7, valinomycin/FCCP, K252a, and rapamycin). A putative W-7 target, calmodulin (Cmd1p), acts late during invagination in a calcium-independent way (Uttenweiler *et al.*, 2005).

In this study we have identified the vacuolar transporter chaperone (VTC) complex as a bona fide Cmd1p target in microautophagy. The VTC complex is enriched at the vacuolar membrane, but also localizes to other cellular compartments (Cohen *et al.*, 1999; Ogawa *et al.*, 2000; Muller *et al.*, 2003). All Vtc proteins contain three C-terminal transmembrane helices. In contrast to Vtc1p, which is small and almost completely embedded in the membrane, Vtc2p, Vtc3p, and Vtc4p possess a large hydrophilic N-terminal domain that faces the cytosol (Muller *et al.*, 2003). Vtc proteins have been implicated in several aspects of membrane transport and vesicular traffic (Cohen *et al.*, 1999; Murray and Johnson, 2000, 2001; Nelson *et al.*, 2000; Muller *et al.*, 2002, 2003). Here, we have used a combination of microscopic and biochemical approaches to test the role of the VTC complex during microautophagy.

MATERIALS AND METHODS

Sources of Chemicals

W-7 and colorimetric chymotrypsin substrate I (Calbiochem, La Jolla, CA), EGTA (Roth, Karlsruhe, Germany), yeast lytic enzyme (ICN Biochemicals, Costa Mesa, CA), α-Chymotrypsin (Sigma, St. Louis, MO), calmodulin sepharose 4B (Amersham Biosciences, Piscataway, NJ), protein A agarose (Roche, Indianapolis, IN), monoclonal mouse anti-His_6-antibody (Qiagen, Chatsworth, CA), Ophiobolin A (Sigma), rapamycin (Alexis, Gruenberg, Germany). Drugs were suspended as 5–100× stock solution in PS buffer (200 mM sorbitol, 10 mM PIPES/KOH, pH 6.8; W-7, EGTA) or DMSO (ophiobolin A, rapamycin, chymotrypsin substrate I) and stored at −20°C.

Yeast Strains

Strain BY4727 (wild type) and corresponding knockout strains OMY20 (Δvtc1), OMY21 (Δvtc2), and OMY22 (Δvtc3) have been described previously (Muller *et al.*, 2003). Wild-type VTC4 and the corresponding Δvtc4 strain were derived from diploid strain BY262 by sporulation: they are the haploid parental strains that had been used for generating Δpep4 strains SBY86 and SBY83 as described before (Muller *et al.*, 2002). Strains Y10000 (BY4742, wild type), Y10212 (Δvtc1), Y17273 (Δvtc2), Y12809 (Δvtc3), Y16780 (Δvtc4), Y15382 (Δatg3), Y13104 (Δatg8), Y15078 (Δego1), Y14793 (Δgtr2), and Y13214 (Δego3) were purchased from Euroscarf (Frankfurt, Germany). Strain K91-1A was kindly provided by Y. Kaneko. Strains DBY5734 (CMD1 wild type), DBY5706 (cmd1-226), DBY5708 (cmd1-228), DBY5713 (cmd1-233), DBY5719 (cmd1-239; Ohya and Botstein, 1994), and CRY1 (CMD1 wild type), IGY149 (cmd1-6), IGY148 (cmd1-5; Geiser *et al.*, 1991) also have been described before. GFP-Pho8p was expressed in wild-type strain DBY5734.

Yeast cells were cultured, and cytosol from strains K91-1A was prepared as described previously (Sattler and Mayer, 2000).

Vacuole preparation was performed as described previously (Sattler and Mayer, 2000), but by using yeast lytic enzyme (from *Arthrobacter luteus*, ICN catalogue number 360944, final concentration: 3.27 mg/ml) or β-1,3-glucanase from *Oerskovia xanthineolytica* (Shen *et al.*, 1991; Nichols *et al.*, 1997; expressed in *Escherichia. coli* strain RSB 805, final concentration 0.67 mg/ml) instead of oxalyticase. For storage of vacuoles, glycerol (10% wt/vol from a 50% stock) was added to a fresh vacuole suspension. The suspension was frozen as little nuggets in liquid nitrogen and stored at −80°C (Kunz *et al.*, 2004).

In Vitro Microautophagy Assay

A standard reaction had a volume of 45 μl and was composed of: vacuoles (0.2 mg/ml, either freshly prepared or thawed from a −80°C stock), 6.8 mg/ml (K91-1A-cells) cytosol from starved cells, 105 mM KCl, 7 mM $MgCl_2$, 2.2 mM ATP, 88 mM disodium creatine phosphate, 175 U/ml (0.463 μg/ml) creatine kinase, 17 μg/ml luciferase, 100 μM DTT, 0.1 mM pefabloc SC, 0.5 mM *o*-phenanthrolin, 0.5 μg/ml pepstatin A, 200 mM sorbitol, 10 mM PIPES/KOH, pH 6.8. This mixture was incubated for 1 h at 27°C. For measuring luciferase uptake the samples were chilled on ice, diluted with 300 μl 150 mM KCl in PS buffer, and centrifuged (6500 × *g*, 3 min, 2°C, fixed angle table top centrifuge). The pellet was washed once more with 150 mM KCl in PS buffer and resuspended in 55 μl 150 mM KCl in PS buffer. Proteinase K was added (0.3 mg/ml from 18× stock) and incubated on ice for 23 min. Digestion was stopped by adding 55 μl 1 mM phenylmethylsulfonylfluoride (PMSF)/150 mM KCl in PS buffer. Luciferase activity was determined using an assay kit according to the manufacturer's instruction (Berthold Detection Systems, Pforzheim, Germany): 25 μl of sample was mixed with 25 μl of lysis buffer, and 50 μl of substrate mix was added directly before counting light emission in a microplate luminometer (LB 96 V, Berthold Technologies, Bad Wildbad, Germany). Alkaline phosphatase activity was determined in a 25-μl aliquot as described previously to serve as an internal reference for the quantity of pelleted vacuoles. Uptake activity was calculated as the quotient of luciferase activity over alkaline phosphatase activity (counts per second/OD_{405} per min) and normalized to an uninhibited standard reaction (60 min, 27°C), which was set to 100%. In some mutant strains the level of mature alkaline phosphatase was different (checked by Western blot or alkaline phosphatase assay; data not shown). When comparing such yeast strains, uptake activity was hence not referred to alkaline phosphatase activity but to the protein content of the vacuoles.

Thin-Section Electron Microscopy

Yeast cells were cryoimmobilized by high-pressure freezing as described previously (Hohenberg *et al.*, 1994). In short, living specimen were sucked into cellulose microcapillaries of 200-μm diameter and 2-mm-long capillary tube segments were transferred to aluminum platelets of 200 μm depth containing 1-hexadecene. The platelets were sandwiched with platelets without any cavity and then frozen with a high-pressure freezer (Bal-Tec HPM 010, Balzers, Liechtenstein). Extraneous hexadecene was removed from the frozen capillary tubes under liquid nitrogen. The frozen capillaries were transferred to 2-ml microtubes with screw caps (Sarstedt no. 72.694) containing the substitution medium precooled to −90°C. Samples for ultrastructural studies were kept in a freeze-substitution unit (Balzers FSU 010, Bal-Tec) in 2% osmium tetroxide in anhydrous acetone at −90°C for 32 h, warmed up to −60°C within 3 h, kept at −60°C for 4 h, warmed up to −40°C within 2 h, and kept there for 4 h. After washing with acetone, the samples were transferred into an acetone-Epon mixture at −40°C, infiltrated at room temperature (RT) in Epon and polymerized at 60°C for 48 h. Samples for immuno/affinity labeling were processed in 0.5% acrolein (WT Vtc4 and Δvtc4) or uranyl acetate (WT Vtc3 and Δvtc3) in anhydrous ethanol using the same temperature/time schedule for freeze-substitution. After washing with ethanol, the samples were transferred into an ethanol-Lowicryl K11M mixture, infiltrated with the polar methacrylate resin Lowicryl K11M (Polysciences, Eppelheim, Germany), and polymerized by UV irradition at −40°C for 48 h. Immunolabeling was done as described previously (Tommassen *et al.*, 1985; van Bergen en Henegouwen and Leunissen, 1986) using affinity-purified antibodies to Vtc3p (N-terminal SPX domain) or to Vtc4p. Anti-Vtc3p (rabbit, 0.5 μg/ml in 0.1% acetylated BSA) and anti-Vtc4p (goat, 3.2 μg/ml in 0.2% gelatin and 0.5% BSA in PBS) were detected via protein A labeled with 15-nm gold particles (the signal for anti-Vtc4p was enhanced with an anti-goat antibody in between). Ultrathin sections, stained with uranyl acetate, were viewed in a Philips CM10 electron microscope at 60 kV.

N-Terminal Tagging of Vtc Proteins with GFP

The genes coding for Vtc1p-Vtc4p were genomically tagged by means of a PCR-based method using the plasmid pYM-N9 (Euroscarf) as described before (Janke *et al.*, 2004). The tagged proteins were expressed at their genomic locus under control of an integrated ADH promotor in the wild-type yeast strain BY4742 (Euroscarf).

Protein Expression

His_6-GST-tagged Vtc domains were expressed in *E. coli* BL21 in LB medium containing 25 μg/ml kanamycin. Expression was induced at OD_{600} = 0.5 with 0.5 mM IPTG (isopropyl-thiogalactopyranoside) for 5 h at 25°C. Cells were lysed on ice by sonication in TBS (50 mM Tris/Cl, pH 8, 0.5% Triton X-100, 150 mM NaCl) protein lysates were cleared by centrifugation (93,000 × g, 20 min, 4°C) and stored as aliquots at −80°C in TBS (50 mM Tris/Cl, pH 8, 0.5% Triton X-100, 150 mM NaCl, 10% glycerol: calmodulin binding assays) or

PS buffer containing 10% glycerol (rescue experiments with vtc knockout strains).

Membrane Preparation

Total membranes were prepared from spheroplasted cells according to the protocol for preparation of vacuoles (see above), using 1 mM PMSF in the spheroplasting buffer. Flotation was carried out for 45 min, and membranes were harvested at a 8%–0% ficoll interface.

Immunoprecipitation

Equal amounts of total membranes (1–2 mg/ml) were solubilized (15 min, 4°C) on a shaker in 50 mM Tris, pH 6.8, 100 mM NaCl, 30 mM CHAPS [3-(3-cholamidopropyl-dimethylammonio)-1-propane-sulfonate] in the presence of 0.1 mM pefabloc SC, 0.5 mM *o*-phenanthrolin, 0.5 μg/ml pepstatin A, and 1 mM $CaCl_2$ or 2 mM EGTA. Solubilizates were centrifuged (20,000 $\times$ *g*, 10 min, 2°C, fixed angle table top centrifuge). Supernatant, 500-1000 μl, was incubated with 20 μl of protein A agarose beads (washed three times in solubilization buffer) and 20 μg of affinity-purified anti-Cmd1p antibodies for 1.5 h at 4°C on a rotator. Beads were washed twice with 500 μl of binding buffer and once with binding buffer without detergent. Proteins were eluted by heating for 10 min at 95°C in sample buffer and separated by SDS-PAGE on a 10–15% gradient gel. Proteins were immunodetected after Western blot to a nitrocellulose membrane.

Binding Assay to Calmodulin Sepharose

Protein lysates (protein concentrations were 3–5 mg/ml, and 8–32 μl were used per tube for binding assay) were diluted in 800 μl of TBS buffer and incubated on a rotator with 20 μl of calmodulin Sepharose beads (washed three times in TBS buffer) in the presence of 2 mM $CaCl_2$ or EGTA for 3 h at 4°C or for 1 h at RT. Beads were washed once with 1 ml of TBS containing 2 mM $CaCl_2$ or EGTA. Proteins were eluted from beads by heating for 10 min at 95°C in sample buffer and separated by SDS-PAGE. Vtc3p was immunodetected after Western blot onto nitrocellulose.

Limited Proteolysis

A 2$\times$ in vitro microautophagic reaction (volume 90 μl, without luciferase) was run in the presence of 50 μM Ca^{2+}. After incubation for 1 h at 27°C, the samples were chilled on ice, diluted with 600 μl 150 mM KCl in PS buffer, and centrifuged (6500 $\times$ *g*, 6 min, 2°C, fixed angle table top centrifuge). The pellet was resuspended in 500 μl of 150 mM KCl in PS buffer. Chymotrypsin was added from a 1 mg/ml stock and the sample was incubated on ice. Digestion was stopped after 10 min by adding 750 μl of chloroforme/methanol mixture (1:2). Precipitated proteins were heated for 10 min at 95°C in sample buffer and separated by SDS-PAGE on a 10% gel. Vtc3p fragments were immunodetected after Western blot to nitrocellulose. Chymotrypsin activity (0.05 mg/ml) was measured by cleaving chymotrypsin substrate I (2 mg/ml from a 5$\times$ stock). The reactions were run in a 96-well microtiter plate (total reaction volume 100 μl) in 150 mM KCl in PS buffer at RT. The cleavage of the substrate was monitored by measuring the increasing absorbance at 405 nm.

RESULTS

Micorautophagy induces vacuolar structures that clearly differ from those seen on rich media. These autophagic tubes show strongly curved membranes at the sites where they invaginate from the vacuolar boundary membrane, an increased lipid to protein ratio toward the tip of the invagination, and fission of membrane vesicles at this tip (Muller *et al.*, 2000). These findings suggested a role for certain lipids or lipid modifying proteins in the overall process. This is plausible considering that the lipid composition determines the spontaneous curvature of lipid bilayers and hence their propensity to form buds or invaginations. In accordance with the suggested role for lipids, low-molecular-weight inhibitors targeting lipid modifying enzymes and lipids had strong effects on microautophagy (Kunz *et al.*, 2004). Because recent findings in our group provide evidence for a role of the VTC proteins in vacuolar lipid metabolism (H. Neumann and A. Mayer, unpublished results), we analyzed whether the VTC complex would be required for the microautophagic invagination process.

We used an in vitro system that allows to quantify microautophagic uptake activity via the uptake of soluble firefly luciferase added to purified vacuoles (Sattler and Mayer, 2000). After the uptake reaction, the vacuoles are reisolated and protease-treated to remove residual luciferase from the vacuolar surface. Microautophagy is then quantified via the luciferase activity protected in the lumen of the vacuoles. We ran the in vitro luciferase uptake assays with vacuoles derived from deletion strains for the four Vtc genes. Vacuoles derived from all four knockout strains showed a significant reduction of microautophagic activity (Figure 1). The most severe reduction was observed for Δvtc1, Δvtc3, and Δvtc4 vacuoles, whereas Δvtc2 vacuoles showed a smaller effect. The different effects of the vtc2 and vtc3 mutations reflect the differential localization of the Vtc proteins (see below) and are due to the existence of isoforms of the VTC complex, one containing only Vtc1p/Vtc3p/Vtc4p and the other one only Vtc1p/Vtc2p/Vtc4p (H. Neumann and A. Mayer, unpublished observation).

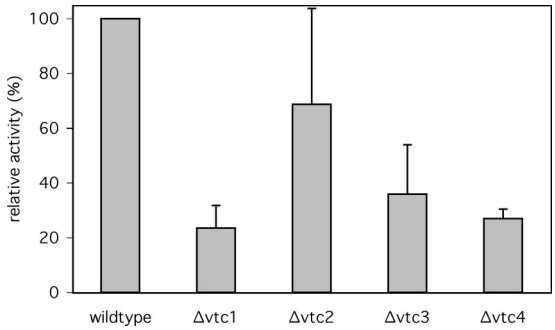

Figure 1. Microautophagic activity of Δvtc vacuoles in vitro. Yeast cells were grown in log phase at 30°C in YPD and vacuoles were prepared at 30°C. In vitro microautophagic reactions were run with cytosol from starved wild-type cells (K91-1A) at 27°C. Data from four to nine independent experiments were averaged. Error bars, SD.

Following an alternative strategy for testing the requirement of Vtc proteins for microautophagic vacuole invagination, we added affinity-purified antibodies to the in vitro assay in order to selectively inactivate Vtc proteins on the surface of wild-type vacuoles. We produced affinity-purified antibodies to Vtc3p and Vtc4p because deletion of Vtc3 and Vtc4 had shown strong effects in the in vitro assay (see Figure 1) and because Vtc1p, although its deletion also produced strong effects, is completely embedded in the membrane and hence barely accessible for antibody binding (Muller *et al.*, 2002, 2003). The resulting antibodies to Vtc3p and Vtc4p were specific for these proteins as tested by Western blotting of vacuolar preparations (Figure 2A). The in vitro reaction was sensitive to affinity-purified antibodies to both Vtc3p and Vtc4p (Figure 2B). Inhibition was not observed with purified bulk antibodies (total IgGs derived from the same animal and prepared after depleting the specific antibodies from the serum by affinity chromatography).

The in vitro assay measures the end point of a microautophagic reaction, the formation of lumenal vesicles. Whether deletion of the Vtc genes already disrupts the ability to form vacuolar invaginations can be tested by quantifying autophagic tubes during starvation by means of fluorescence microscopy. Deletion of either gene had only minor effects on the frequency of autophagic tube formation upon starvation (Figure 3), suggesting that the Vtc proteins should act in autophagic tube organization or vesicle scission rather than in forming the invagination. As a control we used nonstarved cells and *atg* knockout cells which showed reduced tube formation frequencies (Figure 3 and Muller *et al.*, 2000).

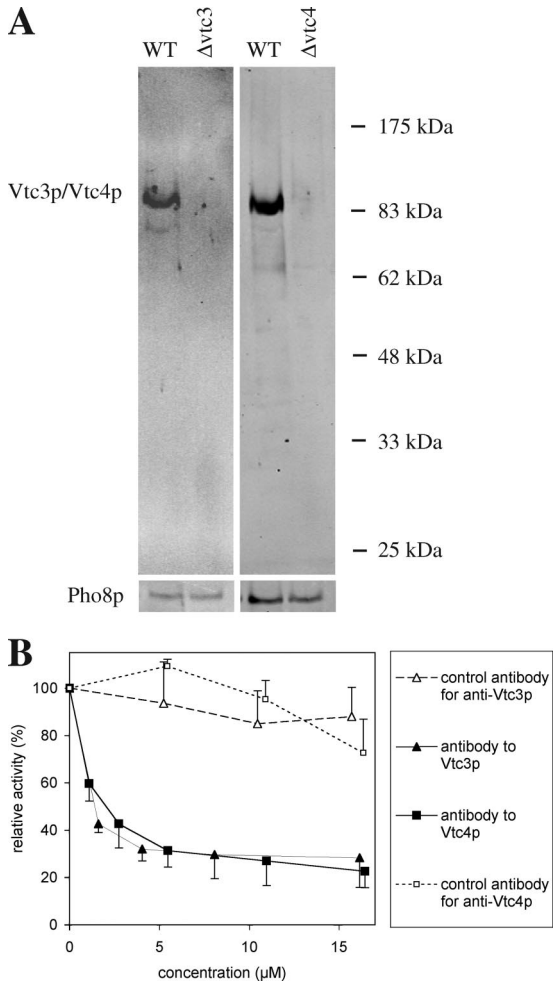

Figure 2. (A) Specificity of affinity-purified antibodies (goat) to Vtc3p and Vtc4p. Vacuolar preparations from wild type or from the respective deletion strains were analyzed by SDS-PAGE and Western blotting with the affinity purified antibodies to Vtc3p or Vtc4p. (B) Sensitivity of in vitro microautophagy to Vtc antibodies. In vitro microautophagic reactions were run with various concentrations of affinity-purified antibodies (goat) to the indicated proteins. Vacuoles were preincubated with antibodies for 10 min on ice before starting the uptake reaction. Control antibodies are total IgG extracted from the sera by adsorption to protein A agarose after the specific antibodies to Vtc3p or Vtc4p had been completely depleted by affinity purification. Data from three independent experiments were averaged. Error bars, SD.

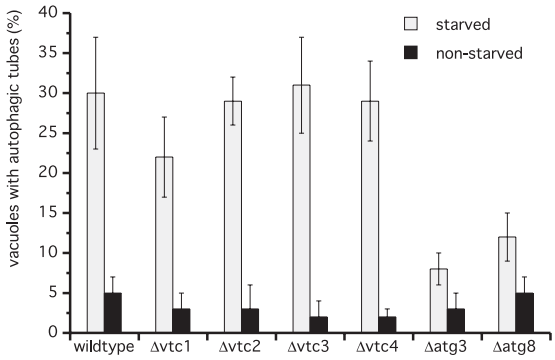

Figure 3. Frequency of autophagic tubes in vtc mutants in vivo. Yeast cells were grown in log phase at 30°C in YPD. Vacuoles were stained with 10 μM FM4-64 for 1 h, washed twice with SD(-N), and starved for 3.5 h in SD(-N) at 30°C. Tube frequencies were determined by fluorescence microscopy. Data from four determinations (200 cells) were averaged.

Large integral membrane proteins are depleted from the tips of autophagic tubes where autophagic bodies pinch off. However, such proteins can be found along the invagination itself (Muller *et al.*, 2000) in a gradient of particle density that is decreasing toward the tip. The VTC complex could thus be located or even enriched at the site of invagination. We tested this by electron microscopy and immunogold labeling of quick-frozen and freeze-substituted yeast cells. Ultrathin sections were stained with antibodies to Vtc3p or Vtc4p (Figure 4A), and the signals on vacuolar membranes and autophagic invaginations were quantified. (Figure 4B). Both Vtc3p and Vtc4p were enriched about twofold on the membranes forming the invaginations versus the vacuolar boundary membrane.

We also analyzed living yeast cells expressing Vtc proteins with GFP-tags at their cytosolic N-termini (because at the C-termini they would be exposed to vacuolar proteinases; Muller *et al.*, 2002). These strains express GFP-Vtc fusion proteins as sole source of Vtc proteins. Vacuoles carrying the GFP-fusions showed considerable activity in the in vitro microautophagic reaction, suggesting that the tagged versions were largely functional for this reaction (Figure 5A). All GFP-Vtc fusions localized to the ER, marking the nuclear rim. In addition, we detected signals of similar strength in a not completely homogeneous pattern at the cell periphery. This should represent either peripheral ER and/or the plasma membrane. While all VTC proteins were detectable on vacuoles, only GFP-Vtc1p/3p/4p (but not GFP-Vtc2p) were enriched on them, in particular at the contact sites between vacuoles (vacuolar interfaces or vertices). On induction of autophagy (either by treatment with rapamycin or shift to SD(-N) starvation medium) the distribution of GFP-Vtc2p did not change significantly. In contrast, GFP-Vtc1p/3p/4p accumulated more strongly at the vacuolar membrane, at the expense of nonvacuolar localizations. In particular GFP-Vtc4p localized almost quantitatively to vacuoles under these conditions (Figure 5B) and became highly enriched also on vacuolar invaginations (Figure 5C). As a control we used cells expressing a GFP-tagged form of another vacuolar membrane protein, the alkaline phosphatase Pho8p (Odorizzi *et al.*, 1998). GFP-Pho8p does not concentrate in invaginations upon treatment with rapamycin (Figure 5C). Thus, Vtc proteins are recruited to the vacuole and also to vacuolar invaginations upon nutrient limitation, supporting their role in microautophagy.

Calmodulin (Cmd1p) has a Ca^{2+}-independent role in microautophagic vacuole invagination (Uttenweiler *et al.*, 2005). It is a 16-kDa protein that in yeast binds three calcium ions via EF hands and simultaneously undergoes a dramatic conformational change (Luan *et al.*, 1987; Matsuura *et al.*, 1991; Starovasnik *et al.*, 1993; Yazawa *et al.*, 1999). Cmd1p is also involved in other cellular processes, such as organization of the actin cytoskeleton (Ohya and Botstein, 1994), chromosome segregation during mitosis (Kao *et al.*, 1990), membrane fusion (Peters and Mayer, 1998; Burgoyne and Clague, 2003), endocytosis (Kubler *et al.*, 1994), and nuclear division (Bachs *et al.*, 1990). Proximity between Cmd1p and Vtc4p had been shown previously by chemical cross-linking (Peters *et al.*, 2001). We hence tested whether the VTC complex could represent a bona fide target of calmodulin for microautophagy. Calmodulin binding often stabilizes proteins, e.g., estrogen receptors (Li *et al.*, 2001); spectrin (Rotter

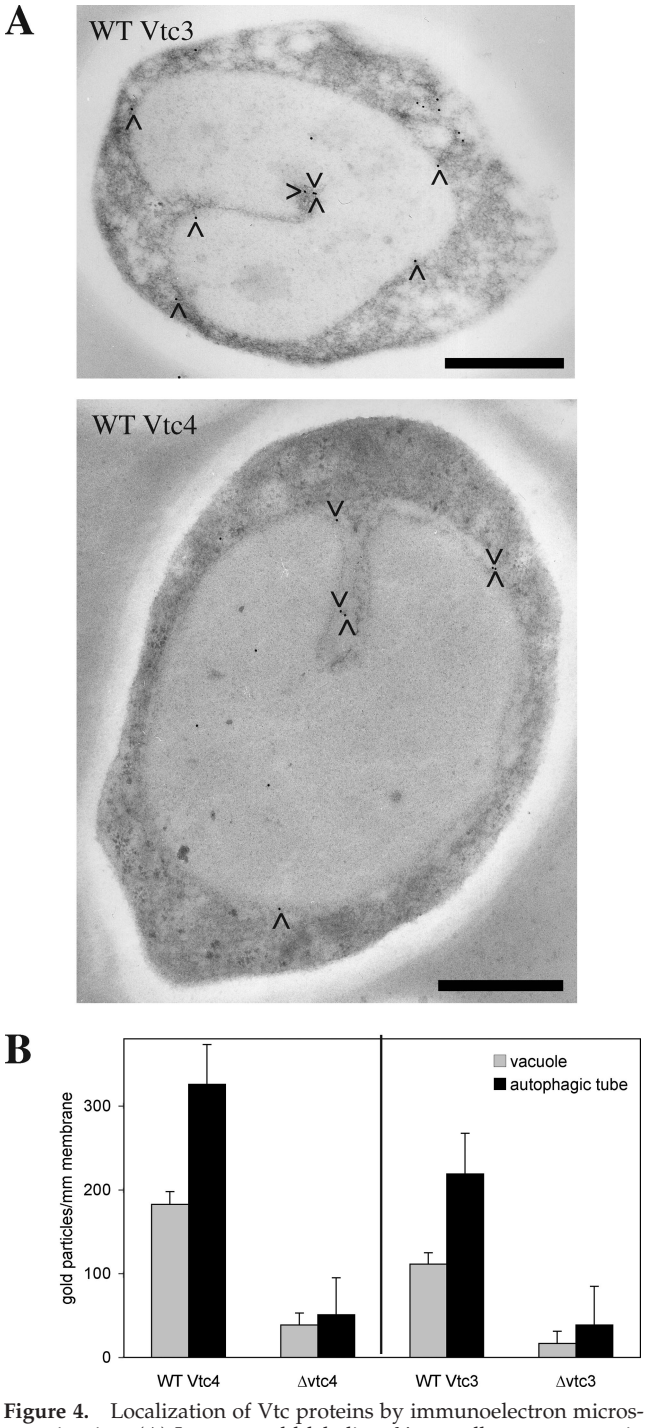

Figure 4. Localization of Vtc proteins by immunoelectron microscopy in vivo. (A) Immunogold labeling. Yeast cells were grown in log phase at 30°C in YPD, washed twice with SD(-N), and starved for 3.5 h in SD(-N) at 30°C. Cells were prepared for electron microscopy by high-pressure freezing and freeze-substitution. Thin sections showing vacuolar invaginations (n = 41 for wild-type Vtc3 and n = 30 for ΔVtc3, n = 31 for wild-type Vtc4 and Δvtc4) were stained with antibodies and protein A-gold. The pictures show two examples of labeled thin sections. (B) Quantitation. Gold particles on the pictures from A were counted along invaginated membranes and on the vacuolar boundary membranes (statistical significances: $p \geq 95\%$ for Vtc3p and $p \geq 99\%$ for Vtc4p). SD for each bar was determined from three data sets of equal size (randomly chosen pictures). Black bars, 1 μm.

et al., 2004); PECAM-1 (Wong *et al.*, 2004); membrane-bound L-selectin (Kahn *et al.*, 1998); growth factor precursors; the receptor tyrosine kinase TrkA; and the β-amyloid precursor (Diaz-Rodriguez *et al.*, 2000). If calmodulin binding influenced conformation or stability of the VTC complex in the membrane, it might be possible to distinguish between these different conformations by limited proteolysis. We tested this hypothesis for Vtc3p by running in vitro uptake reactions in the presence of the calmodulin inhibitors W-7 or ophiobolin A (Leung *et al.*, 1988). At the end of the reaction, vacuoles were washed, treated with chymotrypsin, and analyzed for proteolytic fragments by SDS-PAGE and Western blotting (Figure 6A). In the absence of chymotrypsin almost no fragments of Vtc3p were detectable, indicating that the protein was stable throughout the uptake reaction. A ladder of Vtc3p fragments was generated upon treatment with chymotrypsin. Pretreatment with ophiobolin A increased chymotrypsin sensitivity in comparison to the control sample (no Cmd1p antagonist), whereas W-7 stabilized Vtc3p. The differences in chymotrypsin sensitivity cannot be explained by effects of W-7 or ophiobolin A on the protease because the vacuoles were diluted and washed before limited proteolysis. This can leave only low concentrations of these chemicals during proteolysis (estimated for W-7: <2 μM; ophiobolin A: <0.5 μM) that do not influence chymotrypsin activity, as determined by a colorimetric activity assay run under identical buffer conditions as the proteolysis of the Vtc proteins (see Supplementary Information). In addition we blotted against a membrane-bound internal control protein, the vacuolar t-SNARE Vam3p. Proteolytic sensitivity of Vam3p is not significantly altered by the inhibitors used (Figure 6A).

We also tested whether mutations in Cmd1p might influence VTC stability. Temperature-sensitive (ts) alleles for Cmd1p defined four intragenic complementation groups that affect four different essential calmodulin functions (Ohya and Botstein, 1994). We have chosen one representative ts allele from each complementation group and tested their effect on stability of Vtc3p. Three out of four cmd1 ts mutants showed reduced Vtc3p contents, even if the cells were grown at permissive temperature (Figure 6B). For cmd1-226 the effect became more pronounced upon shift to restrictive temperature. However, cmd1ts vacuoles (except cmd1-233) contained wild-type levels of Vtc3p when cells were grown at permissive temperature, and cells were incubated in the protease inhibitor PMSF before vacuole extraction. Loss of Vtc3p should hence be due to increased proteolytic sensitivity rather than to missorting or reduced expression. At restrictive temperature, Vtc3p in cmd1ts mutants was destabilized even in presence of PMSF.

Because calmodulin was required independently of its ability to chelate Ca^{2+}, we investigated whether the protective effect of Cmd1p on Vtc3p depended on Ca^{2+} binding, using yeast strains expressing calmodulins with strongly reduced Ca^{2+} affinities. These cmd1-5 (E31V, E67V, and E104V) and cmd1-6 (D20A, D56A, and D93A) mutants contain amino acid substitutions in each of the three calcium-binding domains of Cmd1p that remove groups coordinating Ca^{2+} ions (Geiser *et al.*, 1991). Vacuoles from such mutants showed wild-type-like (cmd1-5) or slightly increased Vtc3p levels (cmd1-6) and no signs of proteolytic sensitivity (Figure 6C). Thus, Cmd1p is important for VTC complex stability, and this function does not depend on Ca^{2+} binding.

We tested whether there might be a direct interaction of the VTC complex with calmodulin using purified proteins. The cytosolic parts of Vtc2p, Vtc3p, and Vtc4p consist of an

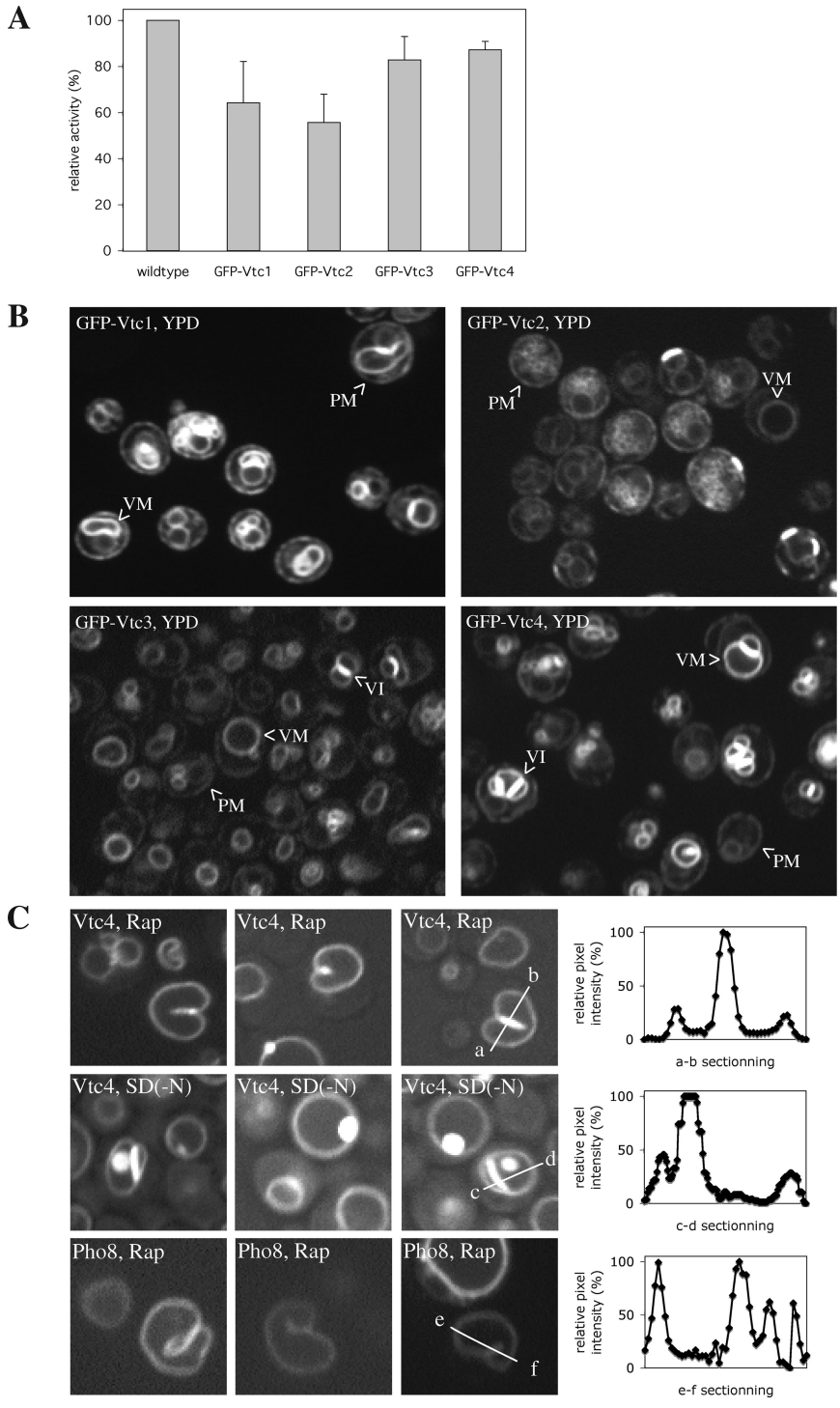

Figure 5. GFP-Vtc proteins. (A) Microautophagic activity of GFP-Vtc vacuoles in vitro. Individual Vtc open reading frames in BY4742 yeast cells were N-terminally tagged by integrating GFP sequences into the genomic locus (Janke *et al.*, 2004), making the tagged proteins the only source of the respective Vtc protein. The tagged open reading frames were expressed under control of a cointegrated ADH promotor. The cells were grown in log phase at 30°C in YPD and vacuoles were prepared at 30°C. In vitro microautophagic reactions were run with cytosol from starved wild-type cells (K91-1A) at 27°C. Data from four to six independent experiments were averaged. Error bars, SD (B and C). Confocal fluorescence microscopy. Yeast cells expressing GFP-Vtc or GFP-Pho8 proteins were analyzed in exponential growth in rich YPD media (B) or after induction of a starvation response (C) by 3 h of incubation in YPD/rapamycin (200 nM) or SD(-N) starvation medium. The GFP signals across the boundary membrane and autophagic tubes were quantified using ImageJ software. PM, plasma membrane; VM, vacuolar membrane; VI, vacuolar interface.

N-terminal SPX domain followed by a large hydrophilic central domain. To test which part of the Vtc proteins supports binding to Cmd1p, we expressed N-terminally His_6-GST-tagged versions of the Vtc domains in *E. coli* and incubated increasing amounts of the cleared protein lysates with Cmd1p-Sepharose. Either central cytosolic Vtc domain (Vtc2p: amino acids 183-553, Vtc3p: amino acids 183-559, and Vtc4p: amino acids 183-487) was soluble and bound to Cmd1p-Sepharose in the presence and in absence of free Ca^{2+}. The N-terminal SPX domain of Vtc4p (amino acids 9-176) did not bind (Figure 7A). The Cmd1p-interaction of the single central Vtc domains expressed in *E. coli* was weakened by ophiobolin A, (Figure 7B) but not by W-7. This is in accord with the differential effects of these compounds on VTC stability. It suggests that Vtc proteins are bona fide targets for calmodulin in microautophagy, and that they can interact directly with calmodulin.

We also tested the calmodulin–Vtc interaction by immunoprecipitation from solubilized membranes using affinity-purified antibodies to Cmd1p. Both Vtc2p, Vtc3p, and Vtc4p

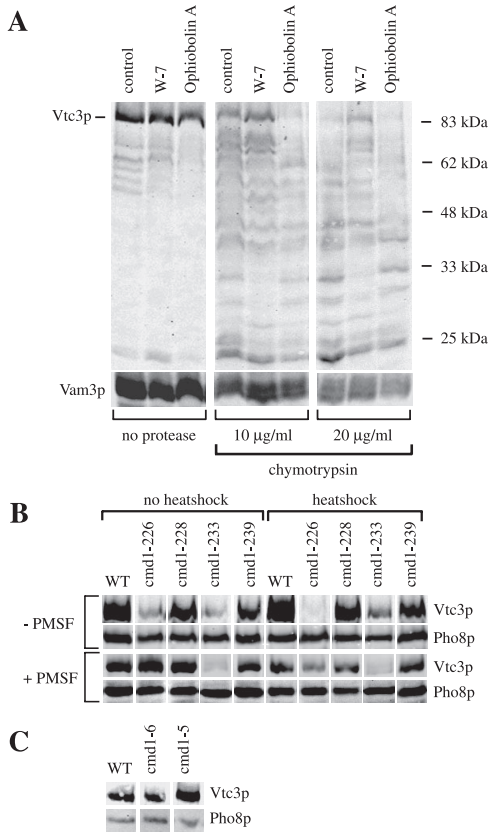

Figure 6. (A) Limited proteolysis of Vtc3p. In vitro microautophagic reactions were run without any inhibitor (control) or with 400 μM W-7 or 100 μM ophiobolin A. After 1 h at 27°C, the reactions were chilled on ice and stopped by dilution with 600 μl 150 mM KCl in PS buffer. Vacuoles were sedimented (6500 × *g*, 6 min, 2°C) and resuspended in 500 μl 150 mM KCl in PS buffer. Chymotrypsin was added to final concentrations as indicated and incubated for 10 min on ice. Digestion was stopped by chloroforme-methanol precipitation. Proteins were analyzed by SDS-PAGE and Western blotting against Vtc3p and the vacuolar SNARE protein Vam3p (control). (B) Temperature-sensitive mutants. Yeast cells were grown in log phase at 25°C in YPD. For heat-shock treatment part of the cultures were transferred to 37°C for 1 h. Cells were harvested and spheroplasted at 30°C (no heat shock) or at 37°C (heat shock) in presence or absence of 1 mM PMSF, and vacuoles were prepared. Vacuoles (50 μg protein) were sedimented (20,000 × *g*, 5 min, 2°C), resuspended in 25 μl of sample buffer, heated to 95°C for 10 min, and analyzed by SDS-PAGE on a 10% gel and Western blotting against the N-terminal SPX-domain of Vtc3p or against the lumenal vacuolar protein Pho8p (alkaline phosphatase) as a loading control. (C) Mutants in the Ca^{2+}-binding sites. Yeast cells were grown in log phase at 30°C in YPD, and vacuoles were prepared at 30°C. Vacuoles (30 μg of protein) were sedimented (20,000 × *g*, 5 min, 2°C), resuspended in 25 μl of sample buffer, heated to 95°C for 10 min, and analyzed as in B.

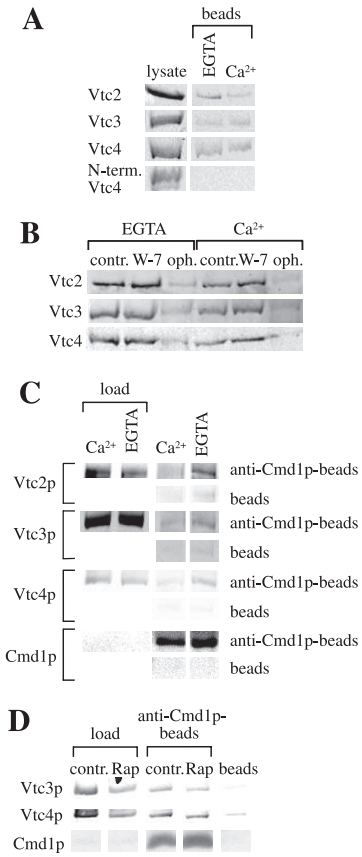

Figure 7. (A) Binding of Vtc central domains to Cmd1p-Sepharose. *E. coli* lysates containing His_6-GST-Vtc domains were incubated with Cmd1p-Sepharose in TBS buffer containing 1 mM EGTA or 1 mM Ca^{2+}. Beads were washed once in binding buffer, and proteins were eluted by heating in sample buffer and analyzed by SDS-PAGE and Western blotting using an antibody to the His_6-tag. The "lysate" lane shows 25% (Vtc2p), 12.5% (Vtc4p and N-term. Vtc4p), or 6.5% (Vtc3p) of the amounts incubated with the beads. (B) Inhibitor sensitivity of Cmd1p binding. *E. coli* lysates containing the central His_6-GST-Vtc domains were incubated with Cmd1p-Sepharose in the presence of 1 mM EGTA or 1 mM Ca^{2+} as in A. The beads had been preincubated for 10 min at room temperature with TBS buffer (control), 400 μM W-7 or 200 μM ophiobolin A (final inhibitor concentrations during adsorption). Proteins bound to the beads were analyzed as in A. (C) Coimmunoprecipitation from native membranes. Total cellular membranes (1–2 mg/ml) derived from a BY4742 wild-type strain were prepared and solubilized in CHAPS. Samples were incubated with 20 μl of protein A agarose beads alone (beads) or protein A agarose beads and 20 μg affinity-purified anti-Cmd1p antibodies (anti-Cmd1p-beads) in the presence of 1 mM Ca^{2+} or 2 mM EGTA for 1.5 h at 4°C on a rotator. The beads were washed and proteins were eluted by heating in sample buffer. Vtc proteins were analyzed by SDS-PAGE and Western blot. Loads are 0.5% (Vtc2p) and 1% (Vtc3p and Vtc4p) of the material incubated with the beads. (D) Coimmunoprecipitation of VTC complex with calmodulin in dependence of rapamycin. Yeast cells were cultured in the presence of 200 nM rapamycin for 3 h at 30°C (control: without rapamycin) and membranes were prepared. Immunoprecipitation was carried out as described in C in the presence of 2 mM EGTA. Vtc proteins were analyzed by SDS-PAGE and Western blot. Loads are 0.5% of the material incubated with the beads.

coimmunoprecipitated with Cmd1p (Figure 7C) in the presence of the Ca^{2+} chelator EGTA, but less in the presence of Ca^{2+}. In line with this, microautophagic uptake in vitro was stimulated by EGTA and inhibited by Ca^{2+} (Uttenweiler *et al.*, 2005 and data not shown). We also tested if the interaction between the Vtc proteins and Cmd1p is regulated by starvation. To this end we coimmunoprecipitated the Vtc proteins with Cmd1p from cells that had been incubated with 200 nM rapamycin (Figure 7D), which mimics starvation conditions. Coimmunoprecipitation was slightly weaker in the rapamycin-treated than in the untreated samples. However, this difference corresponded to a slight decrease of the Vtc content in the rapamycin-treated membranes, suggesting a degradation or lower expression of the Vtc proteins under these conditions. Thus, we found no indication for a regulation of the

Vtc–Cmd1p interaction by starvation. This correlates with our ealier observation that calmodulin appears not to fulfill a Ca^{2+}-dependent regulatory function in microautophagy (Uttenweiler *et al.*, 2005).

The EGO (exit from rapamycin-induced growth arrest) complex (composed of Ego1p, Gtr2p, and Ego3p) is needed for exit from stationary phase after rapamycin treatment and for growth in low rapamycin concentrations (Dubouloz *et al.*, 2005). EGO mutants also show defects in microautophagy. This poses the question whether a defect in microautophagy blocks stationary phase exit or whether microautophagic defects are rather a consequence of the block of stationary phase exit and/or the lack of EGO function. If microautophagy per se were required for stationary phase exit also other mutants with microautopagic defects should show similar phenotypes as EGO complex mutants. Therefore, we tested rapamycin-sensitive growth of VTC and EGO complex mutants. Δvtc cells were spotted onto YPD plates containing 11 nM rapamycin, which is subinhibitory for growth of wild-type cells. All Δvtc strains grew well on low rapamycin, whereas the EGO mutant Δgtr2 did not (Figure 8A). Also in the in vitro system hypersensitivity of the EGO complex knockout strains to rapamycin could not be observed: We ran standard uptake reactions in the presence of increasing concentrations of the drug (up to 25 μM). All EGO complex mutants showed moderately reduced uptake activity (Figure 8B), which was as sensitive to increasing concentrations of rapamycin as that of wild-type vacuoles. In all of the EGO complex mutant vacuoles the content of Vtc3p was reduced in comparison to vacuoles derived from the wild-type strain, even when vacuoles were prepared in the presence of 1 mM PMSF (Figure 8C). The reduced uptake activities correlated well with this reduction in Vtc3p abundance, suggesting that there may not be a direct effect of the EGO complex on in vitro microautophagy under the conditions used.

Our results suggest that the events leading to rapamycin hypersensitivity of cell proliferation in EGO complex mutants may differ from those that are responsible for inhibiting the late steps of microautophagy and that are accessible in our in vitro system. We can reconcile the observed effects with a model in which rapamycin affects two steps of microautophagy: The first one may be an early EGO-dependent signaling event that desensitizes cell proliferation against low rapamycin concentrations. This event precedes microautophagic membrane invagination and may influence stability, abundance and/or activity of the Vtc proteins (and possibly other factors). The second step is fission of autophagic bodies, which is Vtc-dependent and sensitive to high rapamycin concentrations but not directly dependent on the EGO complex. We assume that the early signaling function may not be reproduced by our in vitro system in its present form. It may, however, well be responsible for the effects of the EGO complex on microautophagy and vacuolar Vtc3p abundance in the living cell.

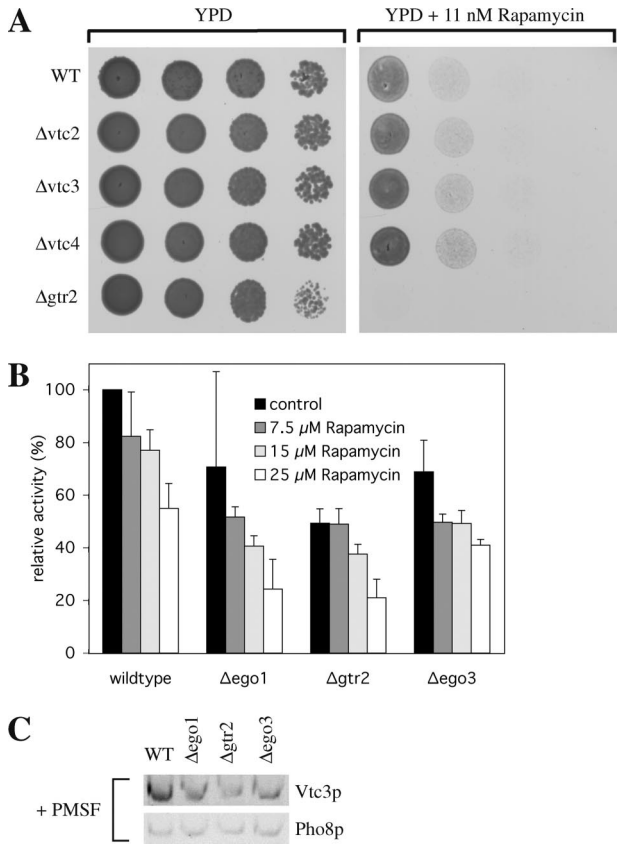

Figure 8. EGO complex mutants. (A) Hypersensitivity to rapamycin. Yeast cells were grown in log phase at 30°C in YPD. Cells were washed twice with H_2O, spotted onto agar plates (series of 10-fold dilutions) containing no inhibitor (YPD) or subinhibitory concentrations (11 nM) of rapamycin and incubated for 2 d at 30°C. (B) Microautophagic activity in vitro. In vitro microautophagy reactions were run without inhibitor (control) or in the presence of different concentrations of rapamycin. Data from three to seven independent experiments were averaged. Error bars, SD. (C) Vtc3p in vacuolar preparations. Yeast cells were grown in log phase at 30°C in YPD and vacuoles were prepared with 1 mM PMSF in the spheroplasting buffer. Vacuoles (33 μg protein) were pelleted (20,000 × *g*, 5 min, 2°C) and analyzed as in Figure 6B.

DISCUSSION

The Vtc proteins form high-molecular-weight complexes that are enriched at the vacuolar membrane, but also localize to other cellular compartments (Cohen *et al.*, 1999; Ogawa *et al.*, 2000; Muller *et al.*, 2003; Figure 5B). Vtc proteins have been implicated in several membrane-related processes, such as sorting of H^+-translocating ATPases, endocytosis, ER-Golgi trafficking, vacuole fusion, and vacuolar polyphosphate homeostasis (Cohen *et al.*, 1999; Murray and Johnson, 2000, 2001; Nelson *et al.*, 2000; Ogawa *et al.*, 2000; Muller *et al.*, 2002, 2003). In this study we demonstrate a role of Vtc proteins for the microautophagic scission of vesicles into the vacuolar lumen.

So far, the question of the physiological relevance of microautophagy could not be definitely answered. The EGO complex is necessary for cells to exit stationary phase after rapamycin treatment (Dubouloz *et al.*, 2005). However, rapamycin treatment in EGO complex knockout cells comes along not only with defects in induction of microautophagy but also with a dramatic decrease of overall protein synthesis (Dubouloz *et al.*, 2005). In addition, recent data show that the EGO complex components have a further role in sorting of the amino acid permease Gap1p (and possibly other proteins) in response to nutrient availability (Gao and Kaiser, 2006). These data in combination with ours suggest that the EGO complex controls multiple cellular processes. Future analyses will be necessary to dissect whether the roles of the EGO complex in microautophagy, in protein synthesis, or in protein sorting cause the defects in recovery after rapamycin treatment. In this work we present mutants (i.e., the VTC complex knockout cells) that are impaired in

microautophagy but still can grow in the presence of the drug rapamycin. The microautophagic process itself may hence be dispensable for leaving the stationary and reentering the exponential growth phase. This suggests that microautophagy could be simply a means to compensate macroautophagic membrane influx after starvation and thereby regulate organellar size and lipid composition rather than being the mechanism responsible for cell recovery after exposure to rapamycin.

The interaction of calmodulin with the VTC complex suggests this complex as a bona fide target of calmodulin for micoautophagic vacuole invagination. We cannot, however, exclude that other calmodulin-binding proteins participate in the reaction. This will require identification and mutation of the calmodulin-binding site on the VTC proteins. This is not trivial because calmodulin can bind its targets in numerous different binding modes that are difficult to predict, as exemplified by the recent cocrystallization of Cmd1p with the adenylyl cyclase domain of CyaA or anthrax edema factor (Guo *et al.*, 2005): 49 residues of CyaA form a network of interactions with 70 residues of calmodulin. Not a single one of these 49 CyaA residues is conserved on endema factor, although both proteins interact with calmodulin via analogous "H helices," which contact the same residues on Cmd1p. Furthermore, there is growing evidence that Cmd1p can bind motifs other than α-helices. Systematic experimental analysis of the Vtc-Cmd1p complex interaction will hence be necessary. Current efforts in the lab to determine the crystal and NMR structure of the Vtc proteins bound to different ligands should be helpful in this regard.

Structural characterization may also resolve the apparent paradoxon that the calmodulin antagonist W-7 inhibits in vitro microautophagy (Uttenweiler *et al.*, 2005) but does not disrupt the Vtc–Cmd1p interaction. Cmd1p might bind Vtc proteins in a conformation that is not influenced by W-7, or W-7 may alter the apo-conformation to partially resemble the Ca^{2+}-loaded state. The latter is not unlikely because Ca^{2+} binding shifts calmodulin from a closed to an open conformation (Kuboniwa *et al.*, 1995; Zhang *et al.*, 1995) creating two hydrophobic pockets (Babu *et al.*, 1985; Kretsinger *et al.*, 1986), which are essential in Ca^{2+}-dependent interactions but not for Ca^{2+}-independent ones (Ikura *et al.*, 1992; Meador *et al.*, 1992, 1993). W-7 binds and blocks these pockets and might, in turn, also stabilize the conformation showing the pockets, thus locking the Vtc–Cmd1p complex in a conformation that partially resembles the Ca^{2+}-bound state. This state is expected to be less active because the presence of Ca^{2+} ions retards rather than stimulates in vitro microautophagy (Uttenweiler *et al.*, 2005).

ACKNOWLEDGMENTS

We thank Christa Baradoy, Ursel Mueller, Brigitte Sailer, Véronique Comte-Miserez, Andrea Schmidt, and Monique Reinhardt for assistance and Trisha Davis, David Botstein, and Randy Schekman for strains and plasmids. This work was funded by grants from the Deutsche Forschungsgemeinschaft (SFB466-A10), BMBF, SNF, and Boehringer Ingelheim Foundation to A.M. and from the Boehringer Ingelheim Fonds to A.U.

REFERENCES

Baba, M., Takeshige, K., Baba, N., and Ohsumi, Y. (1994). Ultrastructural analysis of the autophagic process in yeast: detection of autophagosomes and their characterization. J. Cell Biol. *124*, 903–913.

Babu, Y. S., Sack, J. S., Greenhough, T. J., Bugg, C. E., Means, A. R., and Cook, W. J. (1985). Three-dimensional structure of calmodulin. Nature *315*, 37–40.

Bachs, O., Lanini, L., Serratosa, J., Coll, M. J., Bastos, R., Aligue, R., Rius, E., and Carafoli, E. (1990). Calmodulin-binding proteins in the nuclei of quiescent and proliferatively activated rat liver cells. J. Biol. Chem. *265*, 18595–18600.

Bergamini, E., Cavallini, G., Donati, A., and Gori, Z. (2003). The anti-ageing effects of caloric restriction may involve stimulation of macroautophagy and lysosomal degradation, and can be intensified pharmacologically. Biomed. Pharmacother. *57*, 203–208.

Burgoyne, R. D., and Clague, M. J. (2003). Calcium and calmodulin in membrane fusion. Biochim. Biophys. Acta *1641*, 137–143.

Cohen, A., Perzov, N., Nelson, H., and Nelson, N. (1999). A novel family of yeast chaperons involved in the distribution of V-ATPase and other membrane proteins. J. Biol. Chem. *274*, 26885–26893.

Diaz-Rodriguez, E., Esparis-Ogando, A., Montero, J. C., Yuste, L., and Pandiella, A. (2000). Stimulation of cleavage of membrane proteins by calmodulin inhibitors. Biochem J. *346*(Pt 2), 359–367.

Dubouloz, F., Deloche, O., Wanke, V., Cameroni, E., and De Virgilio, C. (2005). The TOR and EGO protein complexes orchestrate microautophagy in yeast. Mol. Cell *19*, 15–26.

Gao, M., and Kaiser, C. A. (2006). A conserved GTPase-containing complex is required for intracellular sorting of the general amino-acid permease in yeast. Nat. Cell Biol. *8*, 657–667.

Geiser, J. R., van Tuinen, D., Brockerhoff, S. E., Neff, M. M., and Davis, T. N. (1991). Can calmodulin function without binding calcium? Cell *65*, 949–959.

Gozuacik, D., and Kimchi, A. (2004). Autophagy as a cell death and tumor suppressor mechanism. Oncogene *23*, 2891–2906.

Guo, Q., Shen, Y., Lee, Y. S., Gibbs, C. S., Mrksich, M., and Tang, W. J. (2005). Structural basis for the interaction of *Bordetella* pertussis adenylyl cyclase toxin with calmodulin. EMBO J. *24*, 3190–3201.

Gutierrez, M. G., Master, S. S., Singh, S. B., Taylor, G. A., Colombo, M. I., and Deretic, V. (2004). Autophagy is a defense mechanism inhibiting BCG and *Mycobacterium tuberculosis* survival in infected macrophages. Cell *119*, 753–766.

Harding, T. M., Hefner-Gravink, A., Thumm, M., and Klionsky, D. J. (1996). Genetic and phenotypic overlap between autophagy and the cytoplasm to vacuole protein targeting pathway. J. Biol. Chem. *271*, 17621–17624.

Harding, T. M., Morano, K. A., Scott, S. V., and Klionsky, D. J. (1995). Isolation and characterization of yeast mutants in the cytoplasm to vacuole protein targeting pathway. J. Cell Biol. *131*, 591–602.

Hohenberg, H., Mannweiler, K., and Muller, M. (1994). High-pressure freezing of cell suspensions in cellulose capillary tubes. J. Microsc. *175*(Pt 1), 34–43.

Hutchins, M. U., Veenhuis, M., and Klionsky, D. J. (1999). Peroxisome degradation in *Saccharomyces cerevisiae* is dependent on machinery of macroautophagy and the Cvt pathway. J. Cell Sci. *112*(Pt 22), 4079–4087.

Ikura, M., Clore, G. M., Gronenborn, A. M., Zhu, G., Klee, C. B., and Bax, A. (1992). Solution structure of a calmodulin-target peptide complex by multidimensional NMR. Science *256*, 632–638.

Janke, C., *et al.* (2004). A versatile toolbox for PCR-based tagging of yeast genes: new fluorescent proteins, more markers and promoter substitution cassettes. Yeast *21*, 947–962.

Kahn, J., Walcheck, B., Migaki, G. I., Jutila, M. A., and Kishimoto, T. K. (1998). Calmodulin regulates L-selectin adhesion molecule expression and function through a protease-dependent mechanism. Cell *92*, 809–818.

Kao, J. P., Alderton, J. M., Tsien, R. Y., and Steinhardt, R. A. (1990). Active involvement of Ca^{2+} in mitotic progression of Swiss 3T3 fibroblasts. J. Cell Biol. *111*, 183–196.

Kim, J., Dalton, V. M., Eggerton, K. P., Scott, S. V., and Klionsky, D. J. (1999). Apg7p/Cvt2p is required for the cytoplasm-to-vacuole targeting, macroautophagy, and peroxisome degradation pathways. Mol. Biol. Cell *10*, 1337–1351.

Klionsky, D. J., *et al.* (2003). A unified nomenclature for yeast autophagy-related genes. Dev. Cell *5*, 539–545.

Kretsinger, R. H., Rudnick, S. E., and Weissman, L. J. (1986). Crystal structure of calmodulin. J. Inorg. Biochem. *28*, 289–302.

Kubler, E., Schimmoller, F., and Riezman, H. (1994). Calcium-independent calmodulin requirement for endocytosis in yeast. EMBO J. *13*, 5539–5546.

Kuboniwa, H., Tjandra, N., Grzesiek, S., Ren, H., Klee, C. B., and Bax, A. (1995). Solution structure of calcium-free calmodulin. Nat. Struct. Biol. *2*, 768–776.

Kunz, J. B., Schwarz, H., and Mayer, A. (2004). Determination of four sequential stages during microautophagy in vitro. J. Biol. Chem. *279*, 9987–9996.

Leung, P. C., Graves, L. M., and Tipton, C. L. (1988). Characterization of the interaction of ophiobolin A and calmodulin. Int. J. Biochem. *20*, 1351–1359.

Levine, B., and Klionsky, D. J. (2004). Development by self-digestion: molecular mechanisms and biological functions of autophagy. Dev. Cell *6*, 463–477.

Li, Z., Joyal, J. L., and Sacks, D. B. (2001). Calmodulin enhances the stability of the estrogen receptor. J. Biol. Chem. *276*, 17354–17360.

Longo, V. D., and Finch, C. E. (2003). Evolutionary medicine: from dwarf model systems to healthy centenarians? Science *299*, 1342–1346.

Luan, Y., Matsuura, I., Yazawa, M., Nakamura, T., and Yagi, K. (1987). Yeast calmodulin: structural and functional differences compared with vertebrate calmodulin. J. Biochem. (Tokyo) *102*, 1531–1537.

Matsuura, I., Ishihara, K., Nakai, Y., Yazawa, M., Toda, H., and Yagi, K. (1991). A site-directed mutagenesis study of yeast calmodulin. J. Biochem. (Tokyo) *109*, 190–197.

Meador, W. E., Means, A. R., and Quiocho, F. A. (1992). Target enzyme recognition by calmodulin: 2.4 A structure of a calmodulin-peptide complex. Science *257*, 1251–1255.

Meador, W. E., Means, A. R., and Quiocho, F. A. (1993). Modulation of calmodulin plasticity in molecular recognition on the basis of x-ray structures. Science *262*, 1718–1721.

Melendez, A., Talloczy, Z., Seaman, M., Eskelinen, E. L., Hall, D. H., and Levine, B. (2003). Autophagy genes are essential for dauer development and life-span extension in *C. elegans*. Science *301*, 1387–1391.

Mukaiyama, H., Baba, M., Osumi, M., Aoyagi, S., Kato, N., Ohsumi, Y., and Sakai, Y. (2004). Modification of a ubiquitin-like protein Paz2 conducted micropexophagy through formation of a novel membrane structure. Mol. Biol. Cell *15*, 58–70.

Mukaiyama, H., Oku, M., Baba, M., Samizo, T., Hammond, A. T., Glick, B. S., Kato, N., and Sakai, Y. (2002). Paz2 and 13 other PAZ gene products regulate vacuolar engulfment of peroxisomes during micropexophagy. Genes Cells *7*, 75–90.

Muller, O., Bayer, M. J., Peters, C., Andersen, J. S., Mann, M., and Mayer, A. (2002). The Vtc proteins in vacuole fusion: coupling NSF activity to V0 trans-complex formation. EMBO J. *21*, 259–269.

Muller, O., Neumann, H., Bayer, M. J., and Mayer, A. (2003). Role of the Vtc proteins in V-ATPase stability and membrane trafficking. J. Cell Sci. *116*, 1107–1115.

Muller, O., Sattler, T., Flotenmeyer, M., Schwarz, H., Plattner, H., and Mayer, A. (2000). Autophagic tubes: vacuolar invaginations involved in lateral membrane sorting and inverse vesicle budding. J. Cell Biol. *151*, 519–528.

Murray, J. M., and Johnson, D. I. (2000). Isolation and characterization of Nrf1p, a novel negative regulator of the Cdc42p GTPase in *Schizosaccharomyces pombe*. Genetics *154*, 155–165.

Murray, J. M., and Johnson, D. I. (2001). The Cdc42p GTPase and its regulators Nrf1p and Scd1p are involved in endocytic trafficking in the fission yeast *Schizosaccharomyces pombe*. J. Biol. Chem. *276*, 3004–3009.

Nakagawa, I., *et al.* (2004). Autophagy defends cells against invading group A Streptococcus. Science *306*, 1037–1040.

Nelson, N., Perzov, N., Cohen, A., Hagai, K., Padler, V., and Nelson, H. (2000). The cellular biology of proton-motive force generation by V-ATPases. J. Exp. Biol. *203*(Pt 1), 89–95.

Nichols, B. J., Ungermann, C., Pelham, H. R., Wickner, W. T., and Haas, A. (1997). Homotypic vacuolar fusion mediated by t- and v-SNAREs. Nature *387*, 199–202.

Odorizzi, G., Babst, M., and Emr, S. D. (1998). Fab1p PtdIns(3)P 5-kinase function essential for protein sorting in the multivesicular body. Cell *95*, 847–858.

Ogawa, M., Yoshimori, T., Suzuki, T., Sagara, H., Mizushima, N., and Sasakawa, C. (2005). Escape of intracellular *Shigella* from autophagy. Science *307*, 727–731.

Ogawa, N., DeRisi, J., and Brown, P. O. (2000). New components of a system for phosphate accumulation and polyphosphate metabolism in *Saccharomyces cerevisiae* revealed by genomic expression analysis. Mol. Biol. Cell *11*, 4309–4321.

Ohya, Y., and Botstein, D. (1994). Diverse essential functions revealed by complementing yeast calmodulin mutants. Science *263*, 963–966.

Peters, C., Bayer, M. J., Buhler, S., Andersen, J. S., Mann, M., and Mayer, A. (2001). Trans-complex formation by proteolipid channels in the terminal phase of membrane fusion. Nature *409*, 581–588.

Peters, C., and Mayer, A. (1998). Ca^{2+}/calmodulin signals the completion of docking and triggers a late step of vacuole fusion. Nature *396*, 575–580.

Qu, X., *et al.* (2003). Promotion of tumorigenesis by heterozygous disruption of the beclin 1 autophagy gene. J. Clin. Invest. *112*, 1809–1820.

Reggiori, F., and Klionsky, D. J. (2002). Autophagy in the eukaryotic cell. Eukaryot. Cell *1*, 11–21.

Roberts, P., Moshitch-Moshkovitz, S., Kvam, E., O'Toole, E., Winey, M., and Goldfarb, D. S. (2003). Piecemeal microautophagy of nucleus in *Saccharomyces cerevisiae*. Mol. Biol. Cell *14*, 129–141.

Rotter, B., Kroviarski, Y., Nicolas, G., Dhermy, D., and Lecomte, M. C. (2004). AlphaII-spectrin is an in vitro target for caspase-2, and its cleavage is regulated by calmodulin binding. Biochem. J. *378*, 161–168.

Sakai, Y., Koller, A., Rangell, L. K., Keller, G. A., and Subramani, S. (1998). Peroxisome degradation by microautophagy in *Pichia pastoris*: identification of specific steps and morphological intermediates. J. Cell Biol. *141*, 625–636.

Sattler, T., and Mayer, A. (2000). Cell-free reconstitution of microautophagic vacuole invagination and vesicle formation. J. Cell Biol. *151*, 529–538.

Shen, S. H., Chretien, P., Bastien, L., and Slilaty, S. N. (1991). Primary sequence of the glucanase gene from Oerskovia xanthineolytica. Expression and purification of the enzyme from *Escherichia coli*. J. Biol. Chem. *266*, 1058–1063.

Starovasnik, M. A., Davis, T. N., and Klevit, R. E. (1993). Similarities and differences between yeast and vertebrate calmodulin: an examination of the calcium-binding and structural properties of calmodulin from the yeast *Saccharomyces cerevisiae*. Biochemistry *32*, 3261–3270.

Stromhaug, P. E., Bevan, A., and Dunn, W. A., Jr. (2001). GSA11 encodes a unique 208-kDa protein required for pexophagy and autophagy in *Pichia pastoris*. J. Biol. Chem. *276*, 42422–42435.

Takeshige, K., Baba, M., Tsuboi, S., Noda, T., and Ohsumi, Y. (1992). Autophagy in yeast demonstrated with proteinase-deficient mutants and conditions for its induction. J. Cell Biol. *119*, 301–311.

Thumm, M., Egner, R., Koch, B., Schlumpberger, M., Straub, M., Veenhuis, M., and Wolf, D. H. (1994). Isolation of autophagocytosis mutants of *Saccharomyces cerevisiae*. FEBS Lett. *349*, 275–280.

Titorenko, V. I., Keizer, I., Harder, W., and Veenhuis, M. (1995). Isolation and characterization of mutants impaired in the selective degradation of peroxisomes in the yeast *Hansenula polymorpha*. J. Bacteriol. *177*, 357–363.

Tommassen, J., Leunissen, J., van Damme-Jongsten, M., and Overduin, P. (1985). Failure of *E. coli* K-12 to transport PhoE-LacZ hybrid proteins out of the cytoplasm. EMBO J. *4*, 1041–1047.

Tsukada, M., and Ohsumi, Y. (1993). Isolation and characterization of autophagy-defective mutants of *Saccharomyces cerevisiae*. FEBS Lett. *333*, 169–174.

Tuttle, D. L., and Dunn, W. A., Jr. (1995). Divergent modes of autophagy in the methylotrophic yeast *Pichia pastoris*. J. Cell Sci. *108*(Pt 1), 25–35.

Tuttle, D. L., Lewin, A. S., and Dunn, W. A., Jr. (1993). Selective autophagy of peroxisomes in methylotrophic yeasts. Eur J. Cell Biol. *60*, 283–290.

Uttenweiler, A., Schwarz, H., and Mayer, A. (2005). Microautophagic vacuole invagination requires calmodulin in a Ca^{2+}-independent function. J. Biol. Chem. *280*, 33289–33297.

van Bergen en Henegouwen, P. M., and Leunissen, J. L. (1986). Controlled growth of colloidal gold particles and implications for labelling efficiency. Histochemistry *85*, 81–87.

Veenhuis, M., Douma, A., Harder, W., and Osumi, M. (1983). Degradation and turnover of peroxisomes in the yeast *Hansenula polymorpha* induced by selective inactivation of peroxisomal enzymes. Arch. Microbiol. *134*, 193–203.

Vellai, T., Takacs-Vellai, K., Zhang, Y., Kovacs, A. L., Orosz, L., and Muller, F. (2003). Genetics: influence of TOR kinase on lifespan in *C. elegans*. Nature *426*, 620.

Wong, M. X., Harbour, S. N., Wee, J. L., Lau, L. M., Andrews, R. K., and Jackson, D. E. (2004). Proteolytic cleavage of platelet endothelial cell adhesion molecule-1 (PECAM-1/CD31) is regulated by a calmodulin-binding motif. FEBS Lett. *568*, 70–78.

Yazawa, M., Nakashima, K., and Yagi, K. (1999). A strange calmodulin of yeast. Mol. Cell Biochem. *190*, 47–54.

Yuan, J., Lipinski, M., and Degterev, A. (2003). Diversity in the mechanisms of neuronal cell death. Neuron *40*, 401–413.

Yuan, W., Stromhaug, P. E., and Dunn, W. A., Jr. (1999). Glucose-induced autophagy of peroxisomes in Pichia pastoris requires a unique E1-like protein. Mol. Biol. Cell *10*, 1353–1366.

Yue, Z., Jin, S., Yang, C., Levine, A. J., and Heintz, N. (2003). Beclin 1, an autophagy gene essential for early embryonic development, is a haploinsufficient tumor suppressor. Proc. Natl. Acad. Sci. USA *100*, 15077–15082.

Zhang, M., Tanaka, T., and Ikura, M. (1995). Calcium-induced conformational transition revealed by the solution structure of apo calmodulin. Nat. Struct. Biol. *2*, 758–767.